



# Historical reconstruction unveils the risk of mass mortality and ecosystem collapse during pancontinental megadrought

Robert C. Godfree<sup>a,1</sup>, Nunzio Knerr<sup>a</sup>, Denise Godfree<sup>b</sup>, John Busby<sup>a</sup>, Bruce Robertson<sup>a</sup>, and Francisco Encinas-Viso<sup>a</sup>

<sup>a</sup>Commonwealth Scientific and Industrial Research Organization National Research Collections Australia, Canberra, ACT 2601, Australia; and <sup>b</sup>Private address, Narrabri, NSW 2390, Australia

Edited by Nils Chr. Stenseth, University of Oslo, Oslo, Norway, and approved June 14, 2019 (received for review February 4, 2019)

**An important new hypothesis in landscape ecology is that extreme, decade-scale megadroughts can be potent drivers of rapid, macroscale ecosystem degradation and collapse. If true, an increase in such events under climate change could have devastating consequences for global biodiversity. However, because few megadroughts have occurred in the modern ecological era, the taxonomic breadth, trophic depth, and geographic pattern of these impacts remain unknown. Here we use ecohistorical techniques to quantify the impact of a record, pancontinental megadrought period (1891 to 1903 CE) on the Australian biota. We show that during this event mortality and severe stress was recorded in >45 bird, mammal, fish, reptile, and plant families in arid, semi-arid, dry temperate, and Mediterranean ecosystems over at least 2.8 million km<sup>2</sup> (36%) of the Australian continent. Trophic analysis reveals a bottom-up pattern of mortality concentrated in primary producer, herbivore, and omnivore guilds. Spatial and temporal reconstruction of premortality rainfall shows that mass mortality and synchronous ecosystem-wide collapse emerged in multiple geographic hotspots after 2 to 4 y of severe (>40%) and intensifying rainfall deficits. However, the presence of hyperabundant herbivores significantly increased the sensitivity of ecosystems to overgrazing-induced meltdown and permanent ecosystem change. The unprecedented taxonomic breadth and spatial scale of these impacts demonstrate that continental-scale megadroughts pose a major future threat to global biodiversity, especially in ecosystems affected by intensive agricultural use, trophic simplification, and invasive species.**

megadrought | ecosystem collapse | mass mortality | trophic impact | Federation Drought

There is growing evidence that under warming scenarios of 1.5–3 °C above preindustrial levels, the magnitude and extent of drought, and the occurrence of decade-scale megadrought, is likely to increase across most global land areas (1–3). This is of great concern because megadroughts\* have a track record of devastating socioecological systems worldwide both historically (4–6) and within the past century (1, 7) on a continental scale, particularly when exacerbated by anthropogenic processes such as overgrazing, water extraction, and intensive land use. For example, 2 multiannual 20th century droughts, the 1970s to 1980s Sahel drought and the 1930s United States “Dust Bowl,” both caused land degradation, ecosystem decline, and human disruption on a massive scale (1, 8). The severity of these impacts was driven by exceptionally low rainfall and reinforced by coupled edaphic-atmospheric processes linked to intensive agricultural land use and human disturbance (8).

A major question in conservation biology is how native and introduced biota might be affected by increasingly intense, continental-scale megadroughts (CSMs) in the future. Recent studies suggest that the ecological impact of such events is likely mediated primarily through rapid shifts in plant and animal populations and the trophic reconfiguration of associated food webs. These changes can be most severe among primary producer and associated herbivore guilds, such as grazers and browsers of

the African savannah (9–11), but may impact predators more than basal species (12) or affect both (13). There is also some evidence that mass mortality events (MMEs) can play a pivotal demographic role during extreme drought, and that these may be responsible for persistent changes in community structure and even transitions between alternate ecosystem states. However, given that CSMs occur very rarely (1, 5), the magnitude of such impacts, the mechanisms through which they manifest across trophic levels, and the implications for biogeography at regional to biome scales remain poorly understood.

One approach is to use historical sources to reconstruct the impacts of major droughts that occurred in the past. Historical reconstructions have successfully been used to investigate the impact of changing climatic regimes and other drivers on insects (14, 15), disease (16), marine biota (17, 18), bird assemblages (19), and ecosystem transitions in general (20), and the use of such data to guide ecosystem management is growing (21). Newspaper articles are particularly valuable for historical ecology, since they

## Significance

It is thought that extreme, decade-scale megadroughts pose a major future threat to global biodiversity under climate change. However, such events occur rarely and so their capacity to drive ecosystem change remains largely unknown. Here we address this question by reconstructing the impacts of an extreme, historical megadrought period (1891 to 1903) on plant and animal assemblages across the Australian continent. The geographic extent (≥2.8 million km<sup>2</sup>) and taxonomic depth (>45 families) of impacts observed during this event were remarkable and include mass population mortality and broad, bottom-up trophic collapse in multiple subcontinental hotspots. Our work provides insights into the potential pattern and magnitude of ecological change that can occur during continental-scale megadrought.

Author contributions: R.C.G. designed research; R.C.G., D.G., J.B., B.R., and F.E.-V. performed research; R.C.G. and N.K. contributed new reagents/analytic tools; R.C.G., N.K., and F.E.-V. analyzed data; and R.C.G. and F.E.-V. wrote the paper.

The authors declare no conflict of interest.

This article is a PNAS Direct Submission.

This open access article is distributed under [Creative Commons Attribution-NonCommercial-NoDerivatives License 4.0 \(CC BY-NC-ND\)](https://creativecommons.org/licenses/by-nc-nd/4.0/).

Data deposition: The database information has been deposited in CSIRO Data Access Portal, <https://data.csiro.au>, DOI: 10.25919/5d19e24c9969c.

<sup>1</sup>To whom correspondence may be addressed. Email: Robert.Godfree@csiro.au.

This article contains supporting information online at [www.pnas.org/lookup/suppl/doi:10.1073/pnas.1902046116/-DCSupplemental](http://www.pnas.org/lookup/suppl/doi:10.1073/pnas.1902046116/-DCSupplemental).

Published online July 15, 2019.

\*The term “megadrought” is variously used to refer to severe, widespread droughts that are either decade scale (sometimes shorter) or multidecadal in duration. Here we define a megadrought as any decade-scale or longer continental or subcontinental-scale period of severe rainfall deficiencies. In Australia this includes the Federation Drought Period (~1891 to 1903 as defined here), the World War II Drought (~1935 to 1945), and the Millennium Drought (MD; ~1997 to 2009) but excludes many shorter annual to semidecadal droughts (see also *SI Appendix, Fig. S1* and text).

open lines of inquiry about historical events for which little or no other information exists. While data compiled from such sources must be used with caution due to potential bias and nonindependence (22–25), they have been successfully used to reconstruct temporal changes in biota (22, 26, 27) and physical, hydrological, or climatic phenomena (28, 29) that occurred decades to centuries ago. They therefore remain a large but mainly untapped resource for investigating the impact of historical drought and other climatic extremes on populations and ecosystems (e.g., refs. 30 and 31).

In this paper we shed light on these questions by developing an ecoclimatic reconstruction of one of the most severe and geographically extensive megadrought intervals of the past 2 centuries, the Australian Federation Drought period (1891 to 1903; FDP). Record low rainfall (see below) and patterns of agricultural land use during the FDP caused catastrophic soil and vegetation loss across large parts of the continental interior (32, 33); in eastern Australia, the most intense phase of rainfall deficiencies, now known as the iconic 1895 to 1903 “Federation Drought” (FD), marked the first major episode (32) in a multidecadal (1895 to 1945) “Dust Bowl” period (ref. 34, *SI Appendix*, Fig. S1) of persistently low rainfall and severe land degradation. The study period also includes preceding intervals of significant drought in western Australia (1891 to 1892) and subtropical Queensland (1892 to 1893). Given concerns over the recent return of significant drought-induced ecosystem decline and mortality of native biota in Australia (35–37), and the potential increase in scale and severity of future megadroughts (1–3), historical CSMs such as the FDP provide one of the only sources of information available on which to build broad-scale predictive drought models that capture the genesis and development of such processes.

We begin by constructing a continent-wide dataset (38) consisting of >500 biotic impact records (BIRs) extracted from contemporary newspaper articles and other historiographic sources during the years 1890 to 1903. Then, using geocoded data from >60 plant and animal genera, we test for evidence of population mortality and ecosystem collapse during the FDP using trophic reconstruction, statistical modeling, biogeographic network analysis, and spatial models of drought duration and magnitude. We also specifically consider evidence that other landscape-scale processes exacerbated the impact of drought on native and exotic biota, and demonstrate methods for assessing the reliability of historiographic sources for quantifying drought impacts. The exceptional magnitude and breadth of impacts on the Australian biota revealed in our study provide key insights into the potential implications of pancontinental megadroughts for biodiversity conservation under climate change globally.

## Results and Discussion

**Extent and Severity of Drought.** Reconstructed rainfall data (39) show that during the FDP virtually the entire Australian continent was affected by protracted and severe precipitation deficits compared with the long-term average ( $P_{AV}$ ; 1889 to 2015). Semi-to quasidecadal deficits occurred in all arid, semiarid, and subtropical areas between 18° S and 33° S (Fig. 1 *A* and *B*) with  $\sim 5.5 \times 10^6$  km<sup>2</sup> experiencing at least one extreme year with total annual precipitation ( $P_A$ ) less than 50% of the average (i.e.,  $P_A < 0.5P_{AV}$ ; Fig. 1*C*). The most severe deficiencies occurred in the west and north of the continent in 1891 to 1892 and 1894 to 1898 (Fig. 1 *A* and *B*), the eastern subtropics in 1892 to 1893, and then most of eastern Australia in 1895 to 1902 (Fig. 1*B* and *SI Appendix*, Fig. S2). In the latter phase drought severity peaked in November 1901 to October 1902, when  $>1.5 \times 10^6$  km<sup>2</sup> received less than 25% of  $P_{AV}$  and  $>2.5 \times 10^6$  km<sup>2</sup> experienced record low rainfall for the period (Fig. 1*D*). Below-average rainfall persisted in parts of eastern Australia through 1903 before breaking in 1904. The severity of drought during the FDP was exacerbated by

the duration and cumulative magnitude of rainfall deficiencies, which reached 7+ years and >200% of  $P_{AV}$  in some arid and semiarid areas (see below).

Recent reconstructions (36, 40) indicate that 3 major decade-scale drought epochs have occurred in the instrumental record: the (1892) 1895 to 1903 “Federation Drought,” the (1935) 1937 to 1945 “World War II Drought,” and the (1997) 2000 to 2009 “Millennium Drought” (MD) (*SI Appendix*, Fig. S1<sup>†</sup>; dates in parentheses indicate the start date used by some authors). Pre-instrumental (pre-1900) and instrumental reconstructions (40) indicate that the FD (especially 1895 to 1902) was the most geographically extensive of the 3, with more intense rainfall deficiencies across most of the eastern half and north of the continent (the exception being far southern regions; refs. 36 and 40) and a combined intensity and spatial footprint that exceeds that of any Australian drought for at least the past 2 centuries and possibly longer (40). In contrast to the MD, rainfall deficiencies were concentrated in spring and summer (36, 40), when many biota are especially sensitive to the combined effects of drought and heat stress (41), and were particularly extreme during 1896, 1899, 1900, 1901, and 1902 (40). Notably, cool-season deficiencies were also extreme during 1902 (40), which was probably the driest year across the continent during the instrumental record. Rainfall deficiencies during the FD were associated with a sustained period of El Niño activity (the warm mode of the El Niño/Southern Oscillation [ENSO]; refs. 36 and 40) combined with the positive phase of the Interdecadal Pacific Oscillation (IPO; ref. 36) and probably neutral to positive values of the Indian Ocean Dipole (IOD) (36, 40, 42).

Secondary indicators confirm the magnitude of drought impacts on hydrological, edaphic, and agricultural systems, with more than  $3 \times 10^6$  km<sup>2</sup> of pastoral land denuded of groundcover, extremely low river levels, tens of millions of livestock dying from starvation and thirst (33), and wind erosion affecting  $>1 \times 10^6$  km<sup>2</sup> of the arid and semiarid pastoral zone [*SI Appendix*, Fig. S3 and Table S1.1–14 (the number after the decimal refers to the account number in *SI Appendix*, Table S1)]. In the southeastern inland severe dust storms and soil drift occurred regularly, burying fences, buildings, and livestock, and even mobilizing formerly stable sand dunes in parts of the arid zone (43). Social and economic impacts were also severe (*SI Appendix*, Table S1.15–18). Collectively, these data support the view that the scale and severity of the FDP meets or exceeds that of other major global droughts of the past century, such as the Sahel (44) and United States “Dust Bowl” droughts (8).

**Structure and Reliability of Biotic Impact Records.** A total of 541 BIRs were extracted from historical sources between 1891 and 1903. The temporal distribution of spatially unique BIR observations (see *Materials and Methods*) was strongly associated with drought severity in northeastern (NE), southeastern (SE), and western (W) continental areas (*SI Appendix*, Fig. S44). Overall, BIRs occurred most frequently in very dry years, especially 1902 (66% and 49% of all records in NE and SE areas, respectively) and 1891 to 1892 (42% of records in W areas; *SI Appendix*, Figs. S2 and S44) and very rarely if ever in wet years (NE = 0%; SE = 0.4%, W = 3.2% of records). The periods of very high BIR counts in the NE (1899 to 1903) and SE (1897 to 1902) are consistent with intensifying drought conditions during these years (*SI Appendix*, Fig. S2). On the other hand, the large number of counts in 1892 in the SE is anomalous, based on the comparatively mild rainfall deficiencies occurring at this time (*SI Appendix*, Fig. S2).

<sup>†</sup>The reported durations of the Federation, World War II, and Millennium Droughts vary across different sources, due to changing intensity and spatial footprints over time. The duration of the Federation Drought viz., (1892) 1895 to 1903, can be interpreted as 1892 to 1903 in the broadest sense, with the most widespread and intense period occurring in 1895 to 1903.

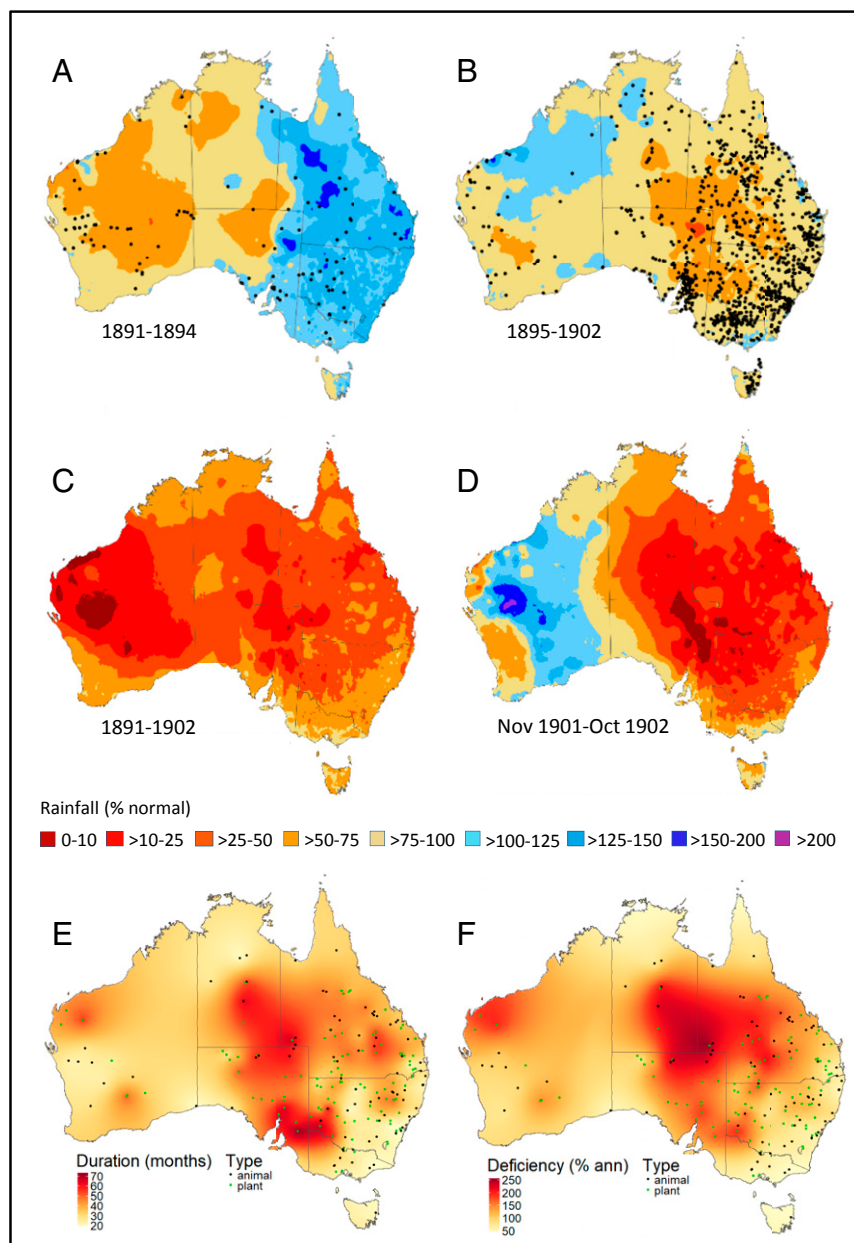


**Fig. 1.** Rainfall patterns and duration and magnitude of drought during the 1891 to 1903 study period. (A) Mean rainfall from 1891 to 1894 as a percentage of the 1889 to 2015 average, showing multi-annual drought in central and western Australia. Black dots indicate geographic locations of drought records during the time period, which partly reflect the pattern of European settlement at the time. (B) As in A except for 1895 to 1902. (C) Minimum annual rainfall as percentage of average, 1891 to 1902. Most of the continent between 18°S and 32°S experienced at least one calendar year with <50% of average annual rainfall. (D) Hyperintense drought between November 1901 and October 1902, with much of eastern Australia receiving <25% of average rainfall. (E) Reconstructed continental profile of drought duration before mortality of biota, defined as the number of preceding months of continuous drought ( $D_{CON}$ ). (F) Continental profile of drought magnitude ( $R_{CON}$ ) before mortality of biota, defined as the cumulative rainfall deficiency over the period  $D_{CON}$  expressed as a percentage of annual mean rainfall  $P_{AV}$ . See *Materials and Methods* for further details.

We constructed a simple index ( $PR_R$ ) to determine association between the timing of a BIR observation and the magnitude of the preceding cumulative 12-mo rainfall relative to average ( $R_{12}$ ; %). Here,  $PR_R$  is the percentile rank of the  $R_{12}$  before the observation month of a given BIR relative to all  $R_{12}$  values in the 1890–1903 study period ( $n = 157$ ). Across all BIRs the mean  $PR_R$  of spatially unique records (see *Materials and Methods*) was 15.6, or in the driest 16% of  $R_{12}$  intervals. Mean  $PR_R$  was also extremely low in the extreme years of 1902 (mean  $PR_R = 5.3$  and 8.7 in the northeast and southeast) and 1891 (5.8 in western parts of the continent). The mean preceding cumulative 12-mo rainfall across all BIRs ( $R_{12} = -45.6\%$ ) was significantly ( $P < 0.001$ ) below the null expectation of  $-4.2\%$  (90% confidence interval =  $-5.0, -3.3$ ), also confirming that BIRs were positively associated with extremely low preceding rainfall. Both are consistent with observer attribution of drought causality. However, the spatial distribution of  $PR_R$  values also reveals a cluster of higher values ( $PR_R > 40$ ) across western New South Wales (NSW) (*SI Appendix, Fig. S4B*). As we discuss below, high  $PR_R$

values identify BIRs in which additional factors may influence the relationship between biotic impact and drought severity.

**Impacts on Animal and Plant Assemblages.** Taxonomic and spatial aggregation of BIR data shows that the FDP caused mortality and extreme stress in a minimum of 50 families (67 genera) of animals and plants (*SI Appendix, Table S2*) over at least  $2.76 \times 10^6$  km<sup>2</sup> or 36% of the Australian continent (*SI Appendix, Fig. S5*), including in 8 of Australia's broad terrestrial ecoregions (45) and 45 of 89 large geographically distinct bioregions (46). Evidence of local (<10 km scale), district (10 to <100 km), or regional (>100 km) population collapse and mass mortality involving hundreds to millions of individuals occurred across much of the continent, with all major animal and plant groups affected (*SI Appendix, Table S3*). To our knowledge the spatial and taxonomic breadth of these impacts exceeds that of any drought yet reported in the Australian or global ecological literature.

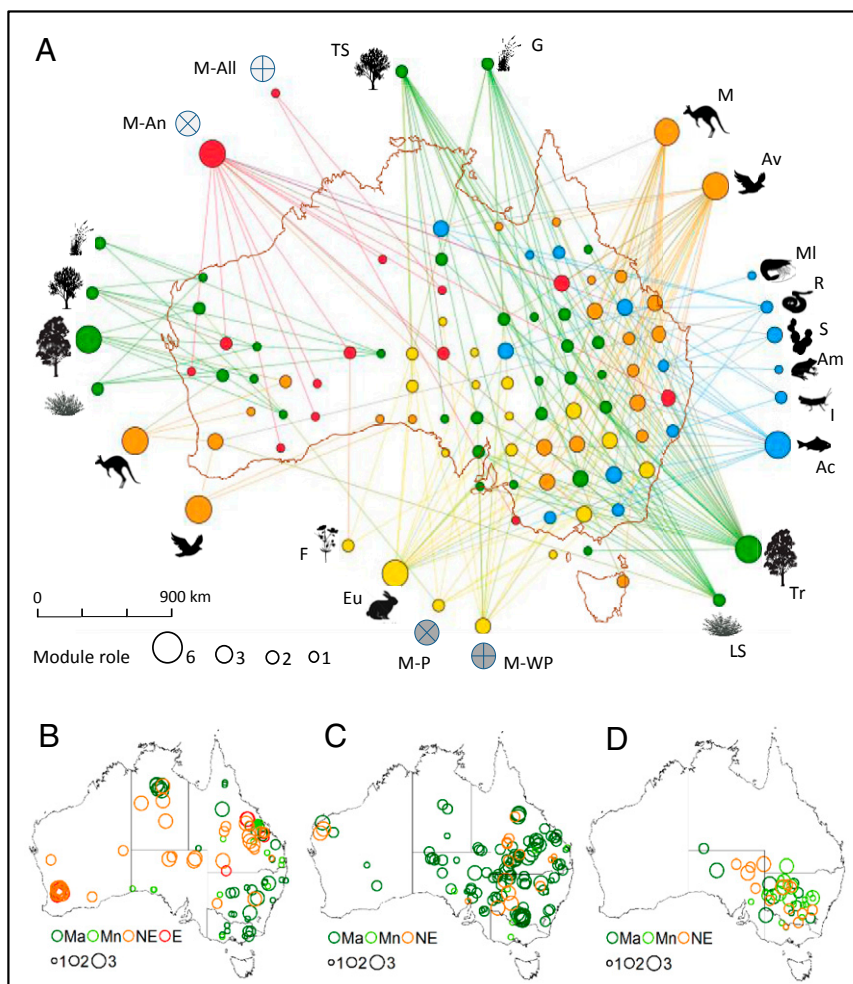


**Fig. 2.** Spatial distribution of drought impacts on flora and fauna during the FDP. (A) Modularity analysis of taxonomic co-occurrence network based on stress and mortality records. Modules are: red = predominately arid zone mixed animal and plant assemblages; green = subtropical to arid woodlands, shrublands, savannas, and grasslands; orange = inland birds and marsupials; blue = fish and minor animal taxa; and yellow = predominantly Mediterranean to arid woody shrubland containing *O. cuniculus* (European rabbit). Module roles: 1) ultra-peripheral node, 2) peripheral node, 3) nonhub connector, and 4) connector hub (49). (B–D) Locations of mass mortality by area (Ma) and number (Mn) and population collapse to near-extirpation (NE) and extirpation (E) for native animals (B), plants (C), and *O. cuniculus* (D). The categories for Ma, NE, and E are as follows: 1 = local (<10 km scale), 2 = district (10 to <100 km) or 3 = regional (>100 km); the categories for Mn are 1)  $10^2$  to  $10^3$ , 2)  $10^4$  to  $10^5$ , and 3)  $10^6$ +. Biotic groups are: Ac = Actinopterygii, Am = Amphibia, Av = Aves, Eu = Eutheria, M = Marsupialia, MI = Malacostraca, I = Insecta, R = Reptilia, F = forbs, G = grasses, LS = low shrubs, TS = tall shrubs, Tr = trees, M-All = mixed all (animal and plant), M-An = mixed animal, M-P = mixed plant, M-WP = mixed woody plant.

We built a co-occurrence network derived from aggregating BIRs into a continental-scale  $100 \text{ km} \times 100 \text{ km}$  co-occurrence grid (47, 48), which is shown in Fig. 2A. Biogeographic patterns within the network helps us to detect geographical hotspots where taxa have been impacted by the drought. Analysis of this network reveals 3 important findings. First, the majority of BIRs were concentrated in drier subtropical, semiarid, and arid parts of the continent (mean annual temperature and precipitation of  $\sim 15$  to  $24^\circ \text{C}$  and 150 to 800 mm, respectively). All major plant and animal groups except for fish and trees display this basic pattern (SI Appendix, Fig. S5A and B), although the total area of impact ( $A_T$ ) for fauna extended slightly further into mesic northern subtropical and southern temperate environments than plants ( $A_T = 2.2 \times 10^6 \text{ km}^2$  vs.  $1.8 \times 10^6 \text{ km}^2$ ; SI Appendix, Fig. S5). Few impacts were reported in more mesic eastern coastal and cool far southern temperate areas of the continent (Fig. 2A), where rainfall deficiencies were less severe (Fig. 1), and also in the monsoonal north, which rainfall reconstructions (Fig. 1, ref. 40) indicate did suffer periods of intense drought. These regions contain numerous centers of high biodiversity and paleo- and neoendemism among major plant and animal lineages (49–51), which suggests that recent megadroughts continue to reinforce continental-scale phylogeographic patterns established during more arid phases of the Pleistocene (52–54).

Second, the high modularity of the network ( $Q = 0.33$ ,  $P = 0.02$ ) indicates strong spatial synchronicity among drought impacts on specific groups of taxa. Here (Fig. 2A), mixed communities (red coloring), woodland, shrubland, and grassland

(green), bird and marsupial assemblages (orange), and fish and minor animal taxa (blue) broadly partition along the strong aridity gradient that extends from coastal through dry temperate and subtropical to semiarid and finally arid central parts of the continent. Semiarid to arid woody shrubland containing invasive populations of *Oryctolagus cuniculus* (European rabbit) form a discrete module (yellow; see below). The biome-scale geographic extent ( $\geq 100,000 \text{ km}^2$ ) of each of these modules suggests that during megadroughts local refugia are likely to play a vital role in maintaining the viability of plant and animal populations, especially in more topographically homogeneous landscapes (55).

Third, the presence of impacted areas involving multiple biotic groups (i.e., nonhub connectors; ref. 47) and local to regional population collapse or mass mortality (Fig. 2B–D) reveals the presence of 2 major subcontinental-scale impact hotspots during the FDP. The most distinct comprised  $\sim 650,000 \text{ km}^2$  of southeastern arid, semiarid, and Mediterranean ecosystems that contained hyperabundant populations of *O. cuniculus* (56) (SI Appendix, Fig. S5A). A trophic reconstruction of BIRs from this hotspot (Fig. 3) shows mortality among herbivore and primary producer guilds, including woody vegetation and herbs, *O. cuniculus*, and native herbivores (*Macropus* spp.). Here, impact records showed a lower level of association with rainfall deficiencies than elsewhere, with the mean  $\text{PR}_R$  of mortality records inside this hotspot being significantly higher than outside (back-transformed adjusted mean  $\text{PR}_R = 16.8$  vs. 8.5;  $F_{1,218} = 6.5$ ,  $P = 0.01$ ), indicating relatively higher rainfall in the preceding 12 mo (viz., driest 17% vs. 9% percentile). However, this mainly reflects

differences among animal records (mean  $PR_R = 21.6$  vs.  $7.3$ ;  $P < 0.001$ ) and not plants (mean  $PR_R = 9.3$  vs.  $7.4$ ;  $P > 0.1$ ). Areas inside this hotspot also had a much higher frequency of impacts attributed to the synergistic effects of drought and overgrazing than outside ( $26\%$  vs.  $6\%$ ; *SI Appendix, Fig. S4C*).

These data support the conclusion that in this hotspot a classical boom-bust dynamic (57) developed during the FDP, which involved a recurring cycle of growth and subsequent collapse and near extirpation of immense (e.g.,  $10^6$  to  $10^7$ ) rabbit populations (Fig. 2D and *SI Appendix, Table S1.36–38*) linked to food and water supply and competition with domestic livestock and native herbivores. In more arid areas, severe drought combined with overgrazing by rabbits and livestock resulted in regional-scale ( $10^2+$  km) mass mortality and collapse of edible shrubs and grasses, especially *Atriplex*, *Maireana*, and *Acacia* spp. The wind erosion, soil drift, and land degradation that followed is a clear case of ecosystem meltdown (58) caused by the interactive effects of an invasive species, extreme drought, predator control, and poor land management (32, 33, 56, 59).

A second area of especially high mortality occurred in central eastern to western Queensland (Qld), which experienced record rainfall deficits in 1901–1902 (Fig. 1D and *SI Appendix, Fig. S2*). In this region a diverse native fauna including large terrestrial macropods, possums, the koala (*Phascolarctos cinereus*), emu (*Dromaius novaehollandiae*), and predatory birds (kookaburra and magpies) suffered apparent population collapse (Fig. 2B and *SI Appendix, Tables S1 and S3*). Mass mortality of vegetation

occurred in stands of vegetation dominated by *Acacia*, *Callitris*, and *Eucalyptus* tens to hundreds of kilometres wide (Fig. 2C and *SI Appendix, Table S1.45–62*). Again, the trophic pattern of these impacts and elsewhere (Fig. 3) indicates a bottom-up, ecosystem-wide cascade of mortality focused on vegetation ( $62\%$  of BIRs) and attenuating across herbivore ( $16\%$ ), omnivore ( $12\%$ ), and mesopredator ( $10\%$ ) guilds. Very few BIRs in this hotspot report overgrazing as a factor leading to biotic stress or mortality (*SI Appendix, Fig. S4C*), indicating that record rainfall deficiencies (up to 75 to 90% below average) were likely the primary driver of mortality. The main exception to this was the catastrophic decline of passerine and some predatory bird populations in central eastern Queensland, which was observationally linked in part to reduced availability of grasses, seeds, and small prey (60), consistent with the response of avian assemblages to drought and livestock overgrazing elsewhere (61).

Mortality in a broad range of taxa was also reported across the western and central arid zone (Fig. 2), although since these areas were sparsely inhabited (*SI Appendix, Fig. S3*), such events were probably underrepresented in our data. Less is known about these impacts, although mass vegetation mortality and severe wind erosion certainly occurred in some areas (e.g., the Gascoyne region of Western Australia; Fig. 2 and *SI Appendix, Fig. S3C*), and native animal populations in the northern deserts (Fig. 2) were apparently so reduced that the food supply of local indigenous human populations was affected (*SI Appendix, Table S1.24*). Livestock grazing was not usually invoked as a causal factor

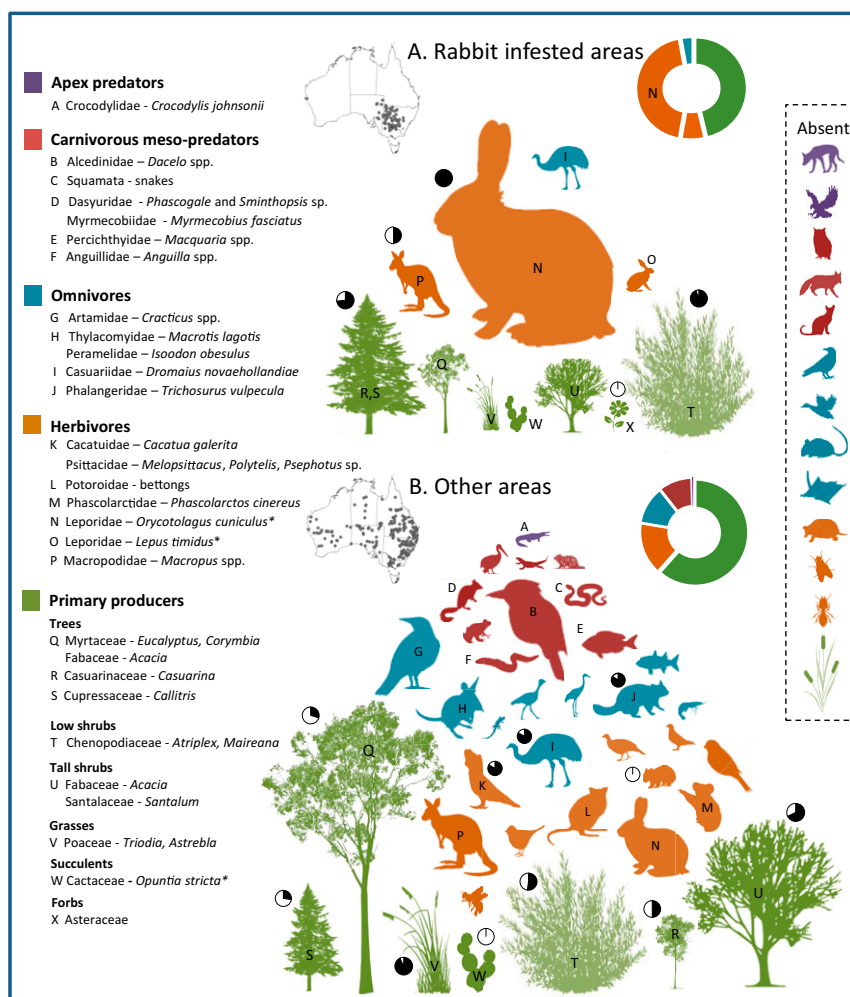


**Fig. 3.** Trophic structure of drought mortality and stress across plant and animal taxa inside (A) and outside (B) areas infested with large populations of the European rabbit, *O. cuniculus*, showing declining impact at higher trophic levels. The size of a minimum circle surrounding each icon is directly proportional to the number of biotic impact records. Pie charts indicate the proportion of mortality records (black) vs. stress records (white). Examples of major groups for which few or no records exist (absent) are provided in each trophic level; from *Top to Bottom*: dingo (*C. familiaris*), raptors, owls, red fox (*V. vulpes*), feral cat (*F. catus*), crows and ravens (Corvidae), waterfowl (especially Anatinae), Muridae, gliders, turtles (especially Chelidae), flies, ants, and aquatic and riparian reeds, rushes, and other plants (including *Phragmites*, *Typha*). \*Introduced species.

(*SI Appendix, Fig. S4C*), although it probably, along with disease, played a contributing role in the sudden decline of native animal populations in the southwestern wheatbelt in 1898–1903 (62) and in vegetation loss across the Gascoyne.

Significant fish-kill events were noted in watercourses and lakes across parts of eastern Australia. Many involved the drying of ephemeral waterholes and lakes, but major inland and coastal rivers were also affected. The magnitude of mortality was often very large, as evidenced by a report that the first steamer to navigate the Darling River in western NSW after it resumed flowing in 1903 pushed up tons of dead fish (*SI Appendix, Table S1.42*). Extremely low water levels, contamination, and eutrophication all probably contributed to mortality (*SI Appendix, Table S1.5–9*), as in more recent drought-driven fish kill events in the Murray-Darling basin (63).

The nature of historical observations, which are often qualitative or semiquantitative, do not usually allow for a strict test of population or ecosystem-level change and recovery over time. However, while acknowledging these limitations, a basic evaluation of the hypothesis that ecosystem collapse occurred across parts of the continent during the FDP is possible. Consistent with recent approaches (64–66), we use 3 general criteria for identifying collapse: 1) a perceived abrupt or drastic decline in biotic populations across multiple trophic levels relative to predrought abundance; 2) a widespread area of impact, not restricted to localized populations associated with local habitat heterogeneity; and 3) decadal-scale (or longer) persistence of these changes. Contemporary articles provide evidence for criteria 1 and 2, while more recent publications referring to the FDP provide data relevant to postdrought recovery (criterion 3).

Collectively, evidence for collapse of semiarid and Mediterranean ecosystems in western NSW, southwest Qld, and eastern South Australia during the FDP is unequivocal. The mass mortality of perennial vegetation (Fig. 2C) and associated loss of soil, biodiversity, and ecosystem function were clearly understood at the time to be catastrophic (*SI Appendix, Table S1.74–76*) and prompted a review of degrading processes in the semiarid Crown Lands of western NSW in 1901 (67). These events are now seen as the first major episode (32, 33) of a longer period of dust bowl conditions and degradation in these regions, which lasted until the mid-1940s (34), when rainfall improved. Only partial recovery has occurred in most affected areas, despite significant improvements to land management practices.

The collapse of bird, mammal, shrub, and tree populations in central eastern to western Queensland (Fig. 2B and C) are also indicative of broad-scale ecosystem collapse. Reports at the time indicate extensive mortality of trees and shrubs from the mesic eastern ranges to the arid interior, many of which appeared to result in the loss of entire cohorts for decades (e.g., *SI Appendix, Table S1.77*). Similarly, there is strong evidence that components of the avifauna in central regions had become rare by 1902, with many taking years or even decades to recover (refs. 60 and 68, *SI Appendix, Table S1.78*). Local to regional extinctions of several species have also been attributed to the event (e.g., ref. 69). Due mainly to remoteness and a low human population at the time, less is known about the magnitude and permanence of FDP impacts in central and western Australia. However, there is strong evidence of severe, widespread decline among faunal assemblages, some apparently permanent, and significant land degradation and soil erosion (typical of ecosystem collapse in eastern Australia) in at least some locations (*SI Appendix, Table S1.45*).

**What Trophic Levels Were Mostly Affected by FDP?** In contrast to other studies (12), our data do not support the hypothesis that drought impacts manifest predominantly at higher trophic levels. Indeed, the near absence of reported mortality among large, conspicuous terrestrial apex and mesopredators, such as dingoes (*Canis familiaris*), feral cats (*Felis catus*), quolls (*Dasyurus* spp.),

raptors, and corvids, is striking (Fig. 3). Newspaper accounts are unlikely to reflect unbiased reporting of underlying ecological phenomena or events, and here we cannot rule out the possibility that mortality in these groups was underreported due to negative social perceptions associated with livestock predation. Indeed, many species, and dingoes particularly, were subjected to population control via bounties and other programs throughout the FDP (59). It is also possible that low reporting rates in these groups reflect lower overall population sizes compared with those in lower trophic levels, or perhaps that drought impacts manifest in predator guilds through reduced fecundity instead of mortality.

On the other hand, numerous accounts attest to the abundance of many predatory species at the time. For example, dingo numbers in parts of inland Australia were reported to be very high due to the availability of rabbits (70), and corvids (i.e., ravens and crows), which attack the eyes and soft tissues of weak livestock, were clearly abundant throughout rabbit-infested and sheep-raising areas. More generally, there is strong evidence that a major pulse in availability of carrion, drought-weakened native animals, rabbits, and livestock supported predator numbers in drought-affected areas (*SI Appendix, Table S1.63–73*), many of which are also facultative scavengers. The lack of mortality among reptiles (especially large taxa such as monitors) may reflect their relatively low metabolic rate per unit of body weight and ability to survive for weeks or months without food or water (71, 72), but, again, at least some were significant predators of rabbits (e.g., monitors) and livestock or scavenged carrion (*SI Appendix, Table S1*).

Our data also show that vegetation impacts were concentrated in dry terrestrial ecosystems (91% of BIRs) and especially prevalent on ridges, hills, and sloping terrain with shallow soils (e.g., *SI Appendix, Table S1.59*). This pattern of topographic development of drought symptoms is consistent with the typical expansion of soil drought from rainfall-dependent habitats of higher relief to lower drainage areas as rainfall deficiencies progress (55), but strikingly different to that observed during the Millennium Drought, which caused extensive mortality of riverine floodplain and wetland species across southeastern Australia (73). These differences are probably linked to the more recent development of hyperdrought associated with anthropogenic water extraction, which now poses a significant additional threat to Australian biota during periods of low rainfall (74, 75).

**Temporal Development of Ecosystem Impacts.** The strongly nonlinear accumulation of impacts among birds, mammals, and woody vegetation (Fig. 4A and B) indicate that populations of these taxa are prone to sudden drought-induced collapse rather than gradual decline (37, 55). Spatial interpolation of preimpact cumulative rainfall data reveals that this typically occurs after 2 to 4 y of continuous drought (drought duration,  $D_{CON}$ ; Fig. 1E) during which cumulative rainfall deficiencies (drought magnitude,  $R_{CON}$ ) total ~80 to 200% of annual mean precipitation (i.e.,  $P_A \sim 0.5$  to  $0.6 P_{AV}$  for the period; Fig. 1F), with the longest and deepest droughts before mortality occurring in arid, central-northern parts of the continent. Similarly, linear models show that  $D_{CON}$  and  $R_{CON}$  were both inversely related to mean annual precipitation ( $P_{AV}$ ) at the BIR impact site ( $P < 0.01$ ; *SI Appendix, Table S4*) with  $D_{CON}$  and  $R_{CON}$  varying from ~29 mo and 80% of  $P_{AV}$  in high rainfall areas ( $P_{AV} = 1,000$  mm) to 36 mo and 120% of  $P_{AV}$  in semiarid ecosystems ( $P_{AV} = 430$  mm; *SI Appendix, Table S4*). These data indicate a higher tolerance among arid-zone species for intense, prolonged drought compared with those found in wetter areas around the continental periphery (Fig. 1E and F), consistent with observed phylogeographic patterns in drought tolerance (76).

In contrast, there was only weak evidence that  $D_{CON}$  and  $R_{CON}$  were lower for native terrestrial animals than for plants (i.e., generally <10 to 20%; *SI Appendix, Table S4*), indicating

that during the FDP these groups tended to undergo mortality following rainfall deficiencies of similar duration and magnitude. A possible exception to this occurred in more peripheral, mesic temperate, and subtropical areas, where animal but not plant mortality was recorded (Fig. 2). However, sample sizes in these habitats were small and associated models significantly affected by spatial autocorrelation (cf., nonspatial and spatial models; *SI Appendix, Table S4*), and so a clear understanding of associated broad taxonomic differences in drought impacts awaits further study. Similarly, differences among specific plant or animal groups were also minor (*SI Appendix, Table S5*), except perhaps for fish, which appeared sensitive to the rapid drying of ephemeral waterbodies and rabbits (see below).

Temporal analysis of drought magnitude (depth)-duration curves data also reveals a pattern of nonlinear intensification of continuous rainfall deficits before mortality of native plants and animals (Fig. 5 *A–D*). These rise from 15 to 30% below normal in years 2 to 4 to ~50% in months 7 through 12 and finally to ~70% in the last 3 preceding months (Fig. 5 *B* and *D*). This terminal period of sharply intensifying rainfall deficits contained, on average, 5 to 8 consecutive months of below average rainfall immediately before mortality ( $D_{\text{CDM}}$ ; Fig. 5 *A–D* and *SI Appendix, Table S4*). For a substantial proportion of BIRs, the period of continuous annual rainfall deficiencies ( $D_{\text{CON}}$ ) before mortality occurred at the end of a period of semicontinuous drought ( $D_{\text{SCO}}$ ) 5 to 8 y long during which mean cumulative rainfall deficits reached 150% of  $P_{\text{AV}}$  or more (Fig. 5 *A–D*). This mainly reflects the high number of BIRs observed during 1902 across eastern Australia following 7 to 8 prior years of generally below average rainfall (i.e., since 1895; Figs. 4 and 5). In northern parts of the continent ( $-16$  to  $-26^\circ$  S) impacts occurred at a similar frequency throughout the year [June to August = 29%, September to November = 29%, December to February = 21%, April to May = 20% of records;  $\chi^2_{(3)} = 1.89$ ,  $P > 0.05$ ]. In contrast, BIRs in southern regions ( $-26$  to  $-42^\circ$  S; excluding rabbits, see below) were most frequent in summer (December to February = 27%) and autumn (April to May = 34%) and least in winter (21%) and spring [18%;  $\chi^2_{(3)} = 14.3$ ,  $P < 0.01$ ]. This is consistent with the summer-dominated nature of rainfall deficiencies during the FDP in this region (40).

Collectively, these data indicate that ecosystems exposed to rapid drought intensification following a semi- to quasidecadal period of persistently accumulating rainfall deficits are at high risk of collapse. Indeed, megadroughts may differ in a fundamental way from droughts of shorter (e.g., annual) duration, with chronic, multiyear rainfall deficiencies allowing the development of mesoscale hydrological and land-cover feedback mechanisms (8) that ultimately render populations and ecosystems more sensitive to intensification of abiotic stress during subsequent extreme years. Examples noted by observers during the FDP include the decline of food resources, development of extreme temperatures, and plant-soil feedback loops caused by the progressive loss of perennial vegetation cover, and the increasingly concentrated impacts of native animals and livestock in refugial waterholes of drying river systems. Such processes indicate that megadrought-landscape interactions exhibit many characteristics of complex adaptive systems, a concept that has proved fruitful in the investigation of other ecological and social phenomena (77).

In our study, habitats containing hyperabundant rabbit populations exhibited a different pattern of impact than elsewhere. Here, impact profiles for most native animal groups, *O. cuniculus*, and woody shrubs (which are herbivorized by rabbits during drought) show punctuated development, beginning after only 1 y of low-intensity drought (1892; Fig. 4C), consistent with a lower degree of association with severe rainfall deficiencies (*SI Appendix, Fig. S4B*). Only trees predominantly suffered impacts in the latest stages of the drought (Fig. 4C). Linear models also support the view that severe rabbit infestation reduced mean

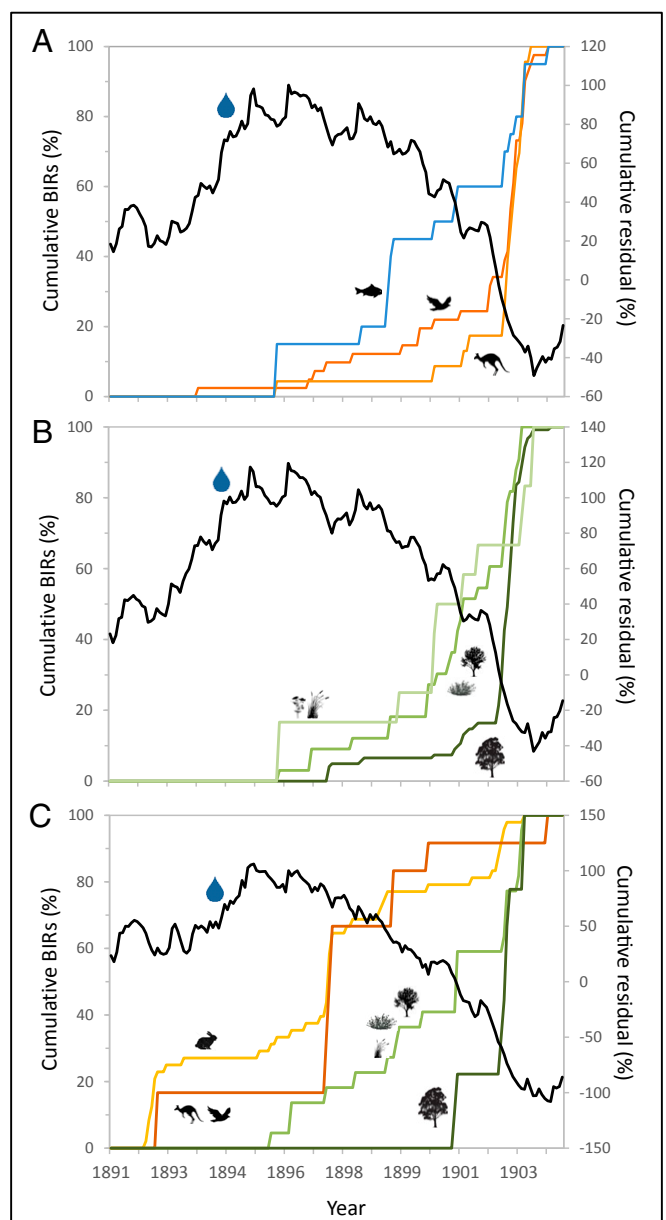


**Fig. 4.** Relationships between cumulative impact (percentage of total BIRs) of major taxonomic groups and rainfall across eastern Australia during the 1891 to 1903 study period outside (*A* and *B*) and inside (*C*) areas heavily infested by European rabbits. Cumulative rainfall residuals (heavy black lines) show above average rainfall between 1891 and 1894 in all areas, apart from a short period in late 1891 to early 1892, followed by establishment of semicontinuous drought in 1895 and continuous drought from 1898 to early 1903 (the Federation Drought; see *Materials and Methods*). The cumulative rainfall residual (relative to the 1889 to 2015 mean) is expressed as a percentage of mean annual rainfall; for example in *C* the cumulative rainfall residual for the period 1895 to 1903 was close to 200% of mean annual rainfall. Icons are as in Fig. 2.

$D_{\text{CON}}$  and  $R_{\text{CON}}$  for some co-occurring native plant and animal groups (by 10 to 12 mo and 30 to 45%, respectively) compared with non- or less-infested areas (Fig. 1 *E* and *F* and *SI Appendix, Tables S4* and *S5*), although spatial models indicate that the impact of other variables (e.g., vegetation, soil types, stocking regimes) cannot be ruled out as contributing to these differences. The frequency of rabbit mortality BIRs in this region was least during winter (June–August = 5%) and spring (September to

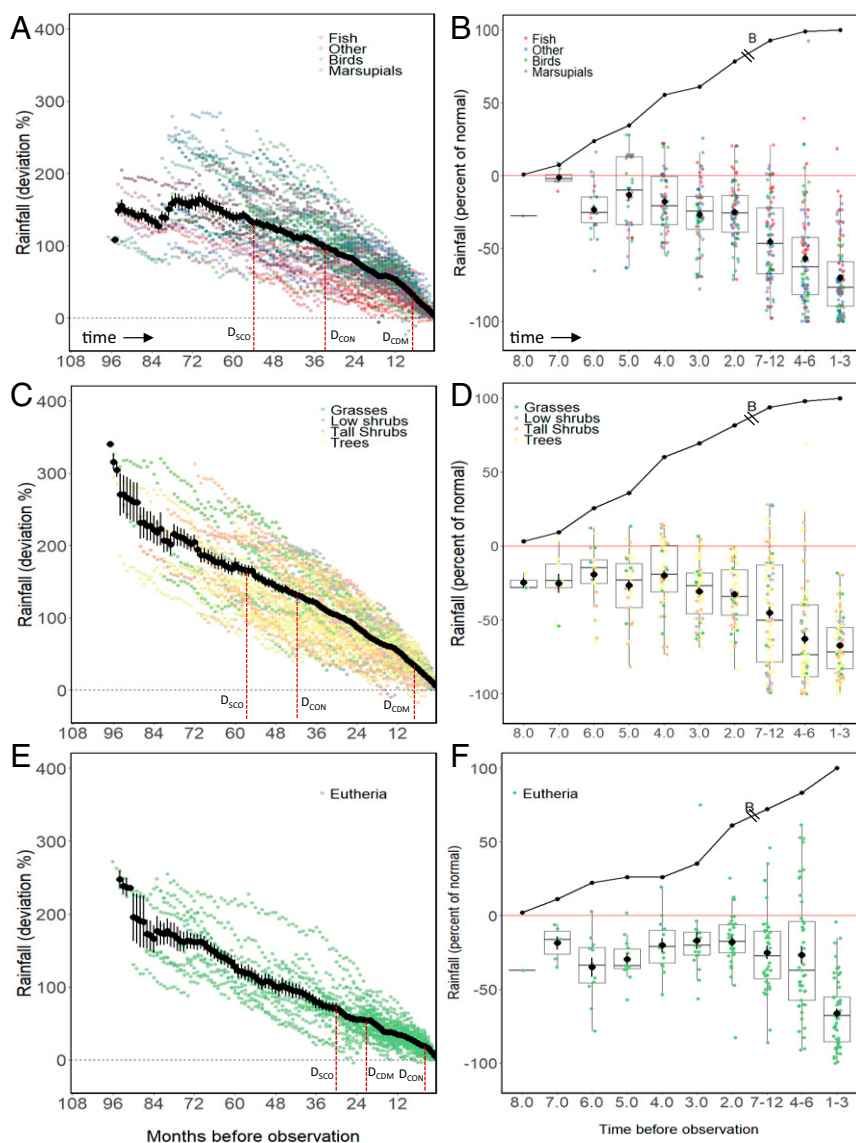


**Fig. 5.** Reconstructed rainfall patterns before mortality in native animals, native plants, and the European rabbit (*O. cuniculus*). (A) Cumulative rainfall deficit as a percentage of mean annual precipitation before mortality in birds, fish, marsupials, and other native animals outside of rabbit-infested areas. Shown are mean values of  $D_{CDM}$  = months of consecutive below average precipitation,  $D_{CON}$  = months of continuous drought, and  $D_{SCO}$  = months of semi-continuous drought. (B) Rainfall deficits for birds, fish, marsupials, and other native animals in months 1 to 3, 4 to 6, 7 to 12, and years 2 through 8 before observed mortality. The solid black line indicates the cumulative count of BIR records as a percentage of the total at each time period. (C and D) As in A and B but for native plant groups (grasses, low shrubs, tall shrubs, trees). (E and F) As in A and B but for *O. cuniculus* inside heavily rabbit infested areas. Data for each BIR extend back in time only to terminal  $D_{CDM}$ ,  $D_{CON}$ , or  $D_{SCO}$  dates. The mean cumulative rainfall deficit value (y axis) can be determined for any period before the BIR observation.

November = 14%) and highest in summer (December to February = 26%) and autumn [March to May = 56%;  $\chi^2_{(3)} = 25.6$ ,  $P < 0.001$ ], suggesting that rabbit populations, which grew during the very wet years of 1889 to 1891 (and probably 1894) to levels vastly in excess of the long-term carrying capacity, collapsed (in 1892 to 1893 and 1895 to 1896; Fig. 4C) following progressive summer–autumn drying and a lack of cool-season herbage growth on which they depend (56).

More generally, these data indicate that assemblages dominated by a hyperabundant, highly fecund herbivore guild are extremely sensitive to drought-induced meltdown, as in other systems lacking robust top-down control (58). This suggests that the progressive trophic downgrading of ecosystems under modern anthropogenic land use regimes globally (78) now poses a significant additional risk to biodiversity in megadrought-prone areas.

## Conclusions

This study shows that it is possible to reconstruct the spatial, taxonomic, trophic, and demographic impacts of historical droughts on biota using analysis of data compiled from contemporary written accounts. The unprecedented geographic extent, taxonomic breadth, and temporal distribution of population mortality and ecosystem collapse that occurred during the Australian Federation

Drought period show that extreme, semi- to decadal megadrought events can have serious demographic and biogeographic consequences for plant and animal populations on a pancontinental scale. These include rapid, broad scale mass biotic mortality and collapse of both agriculturally modified and natural ecosystems. Importantly, our study also indicates a clear bottom-up effect where lower trophic levels (e.g., plants and herbivores), and not higher trophic levels, can be most affected by decadal droughts of this magnitude and duration.

The longest and most intense droughts in eastern Australia (e.g., Federation, WWII, and Millennium droughts) can be largely explained by the modular states of a relatively small set of underlying climatological drivers (e.g., ENSO, IOD, IPO, and the southern annular mode, SAM), albeit manifesting with different spatial and seasonal footprints (36, 40, 42). The periodic recurrence of such events during the 20th century, combined with an apparent shift toward reduced moisture availability across eastern Australia since the mid-19th century (40, 79) and the return of generally drier conditions, rising temperatures, and reduced water availability and runoff in parts of Australia over the past 2 decades (80–82) all suggest that the likelihood of a similar, or possibly even more extreme bioclimatic event occurring in the future is high. More generally, our study shows that an

increase in the frequency and severity of megadroughts clearly poses a serious threat to global biodiversity conservation, especially in tropically downgraded and overgrazed ecosystems.

## Materials and Methods

**Database Development.** The primary source of data consisted of digitized newspaper articles contained in the National Library of Australia's Trove platform (<https://trove.nla.gov.au/>). We conducted a series of searches of Trove that contained the terms *drought*, *dead* or *dying*, followed by 1 of 296 terms or phrases relating to geographic locations or features across all 6 Australian states and 2 territories (mainly towns, rivers, major geographic regions, and telegraph or private stations) or broad vegetation groups, plant genera, and colloquial plant names. Based on these searches we screened >35,000 relevant newspaper articles (and a small number of related explorer journals and other sources) for those documenting either an impact of drought on plants or nondomestic animals (BIRs) or a significant event or attribute of drought-affected areas (drought impact record; DIR). A total of 1,748 DIRs and 541 BIRs with suitable geographic information were identified.

For BIRs, we then extracted information for the following data fields (e.g., *SI Appendix, Fig. S6*): 1) estimated observation date (usually last full calendar month before each report's publication date), 2) broad morphotaxonomic group (8 animal and 6 plant groups, see *SI Appendix, Table S2*), 3) taxonomic identity (family, genus, or species), 4) impact type (mortality or absence, stress), 5) geolocation (latitude, longitude), 6) estimated extent of impact (circle of radius  $r$  in km), 7) Interim Biogeographic Regionalization for Australia (IBRA) bioregion (48), 8) ecosystem type (aquatic, terrestrial, mixed, other), 9) presence of livestock-related factors contributing to the stated impact, 10) location relative to area of severe rabbit infestation in 1891 (RIA; based on ref. 56), and 11) evidence of population collapse or mass mortality. This was classified into 1 of 4 categories: 1) extirpation of population (E), 2) near-extirpation (NE), 3) mass mortality based on area (Ma), and 4) mass mortality based on numerical estimate (Mn). Categories 1 through 3 were then classified as local (hundreds of meters to <10-km radius), district (10- to <100-km radius), or regional (>100-km radius). We classified the Mn category into 1) hundreds to thousands ( $10^2$  to  $10^3$ ), 2) tens to hundreds of thousands ( $10^4$  to  $10^5$ ), and 3) millions or more ( $10^6+$ ).

For DIRs we estimated the geolocations of observations of 1) dust storms, sand storms, and drift, 2) livestock death, 3) hydrological impacts (low water levels in rivers, lakes, etc.), 4) bare understorey, and 5) general drought conditions. Further methodological details are provided in *SI Appendix, SI Text*.

**Rainfall Data and Association with BIRs.** Rainfall data were obtained from the public SILO enhanced climate database (daily rainfall 1889–) hosted by the Science Delivery Division of the Department of Science, Information Technology, and Innovation (DSITI) found at <https://legacy.longpaddock.qld.gov.au/silo/>. We then determined, for Australia, 1) mean annual precipitation ( $P_{AV}$ ; 1889–2015), 2) total annual precipitation  $P$  (all years 1890–1903), 3) percentile annual  $P$ , 4) total  $P$  as a percentage of the mean, and 5) lowest annual  $P$  as total and as percentage of  $P_{AV}$ . We compared numbers of BIRs across “wet” years and “other” years in 3 continental regions (western, northeastern, and southeastern; *SI Appendix, Fig. S4A*) using simple  $\chi^2$  contingency analyses. To avoid dependency among data points we included only BIRs with unique spatial coordinates and observation dates ( $n = 339$ ) in these analyses.

We used analysis of cumulative sum of monthly rainfall residuals ( $R$ ) to quantify the depth and magnitude of drought for each BIR between the last full calendar month before each report date and January 1889. We deter-

mined the preceding duration (in months) of 1) consecutive below average monthly rainfall ( $D_{CDM}$ ), 2) continuous drought ( $D_{CON}$ ; no unbroken 12-mo period of above average rainfall), and 3) semicontinuous drought ( $D_{SCO}$ ; no unbroken 24-mo period above average rainfall). Drought magnitude after  $D_{CON}$  was defined as the total cumulative rainfall residual over the period ( $R_{CON}$ ; percentage of mean annual rainfall). A worked example is provided in *SI Appendix, Fig. S7*.

We also developed a percentile-based index, ( $PR_R$ ), to determine the strength of association between the magnitude of cumulative 12-mo rainfall ( $R_{12}$ , percentage deviation relative to the 1889–2015 average) and the estimated observation date of a given biotic impact record. We determined  $PR_R$  as the percentile rank of  $R_{12}$  before the BIR observation date relative to all cumulative 12-mo rainfall intervals between January–December 1890 and January–December 1903 ( $n = 157$ ; details provided in *SI Appendix, SI Text*).  $PR_R$  was also compared (using BIRs with unique spatial coordinates) both within and outside the primary rabbit infested area (RIA) using generalized least squares linear model analysis. Spatial autocorrelation was accounted for by incorporating an exponential correlation structure which had the lowest Akaike information criterion (AIC) among tested structures (*SI Appendix, SI Text*). We also tested whether the mean  $R_{12}$  across all BIRs differed from a statistical null model using the standard  $z$  statistic.

We also compared the frequency of BIRs citing livestock impact across rabbit-infested and other areas, and across winter, spring, summer, and autumn seasons in the RIA and other northern and southern regions using simple  $\chi^2$  contingency analyses.

## Density and Network Analyses, Spatial Interpolation, and Statistical Modeling.

Kernel density analysis with a bandwidth ( $H$ ) of 5 was performed on geocoded mortality records for key animal and plant groups using the R package GISTools (v. 0.7-4). Modularity network analysis of the network based on spatial co-occurrence of broad impacted plant and animal groups was conducted based on stochastic simulated annealing algorithm using the package netcarto (see ref. 47 for details). Significance of the observed modularity was tested using a randomization test with  $n = 1,000$  replicates implemented in the netcarto command line program (<https://bitbucket.org/amarallab/network-cartography>). Spatial interpolation of  $D_{CON}$  and  $R_{CON}$  was performed using variogram fitting and ordinary kriging approaches (83, 84) and relevant functions in R packages gstat v. 1.1-6, sp v. 1.2-4, and raster v. 2.5-8.

We determined mean values of  $D_{CDM}$ ,  $D_{CON}$ ,  $R_{CON}$ , and  $D_{SCO}$  before mortality for key animal and plant groups. Each parameter was then modeled using generalized least squares linear model analysis with broad biotic group (native animals vs. plants), RIA, and mean site precipitation as predictor variables. Three model types were used: 1) full, nonspatial containing all observations (FNS); 2) full, but incorporating spatial autocorrelation (FS); and 3) restricted nonspatial model using only BIRs with unique geolocations (RNS). For FS models, we tested 5 autocorrelation structures (exponential, Gaussian, linear spatial, rational quadratic, and spherical) and selected the model with the lowest AIC. Model parameters including adjusted means and tests of main effects were constructed and extracted using R packages stats v. 3.4.2 and nlme v. 3.1-139. Further information is provided in *SI Appendix, SI Text*.

**ACKNOWLEDGMENTS.** We acknowledge David Marshall for assistance with sourcing historical records, the staff at the National Library of Australia, the Hay Historical Society for assistance with sourcing and identifying historical photographs, Murray Fagg for helpful discussion, and two anonymous reviewers for helpful comments on versions of the manuscript.

- G. Naumann *et al.*, Global changes in drought conditions under different levels of warming. *Geophys. Res. Lett.* **45**, 3285–3296 (2018).
- T. Zhao, A. Dai, The magnitude and causes of global drought changes in the 21st century under a low-moderate emissions scenario. *J. Clim.* **28**, 4490–4512 (2015).
- C. Prudhomme *et al.*, Hydrological droughts in the 21st century, hotspots and uncertainties from a global multimodel ensemble experiment. *Proc. Natl. Acad. Sci. U.S.A.* **111**, 3262–3267 (2014).
- D. W. Stahle *et al.*, Major Mesoamerican droughts of the past millennium. *Geophys. Res. Lett.* **38**, L05703 (2011).
- B. I. Cook, J. E. Smerdon, R. Seager, E. R. Cook, Pan-continental droughts in North America over the last millennium. *J. Clim.* **27**, 383–397 (2014).
- N. P. Evans *et al.*, Quantification of drought during the collapse of the classic Maya civilization. *Science* **361**, 498–501 (2018).
- C. K. Folland, T. N. Palmer, D. E. Parker, Sahel rainfall and worldwide sea temperatures, 1901–85. *Nature* **320**, 602–607 (1986).
- B. I. Cook, R. L. Miller, R. Seager, Amplification of the North American “Dust Bowl” drought through human-induced land degradation. *Proc. Natl. Acad. Sci. U.S.A.* **106**, 4997–5001 (2009).
- E. Gandiwa, I. M. Heitkönig, P. H. Eilers, H. H. Prins, Rainfall variability and its impact on large mammal populations in a complex of semi-arid African savanna protected areas. *Trop. Ecol.* **57**, 163–180 (2016).
- C. Foley, N. Pettorelli, L. Foley, Severe drought and calf survival in elephants. *Biol. Lett.* **4**, 541–544 (2008).
- K. M. Dunham, The effect of drought on the large mammal populations of Zambezi riverine woodlands. *J. Zool. (Lond.)* **234**, 489–526 (1994).
- M. E. Ledger, L. E. Brown, F. K. Edwards, A. M. Milner, G. Woodward, Drought alters the structure and functioning of complex food webs. *Nat. Clim. Chang.* **3**, 223–227 (2013).
- L. R. Prugh *et al.*, Ecological winners and losers of extreme drought in California. *Nat. Clim. Chang.* **8**, 819–824 (2018).
- H. Tian *et al.*, Reconstruction of a 1,910-y-long locust series reveals consistent associations with climate fluctuations in China. *Proc. Natl. Acad. Sci. U.S.A.* **108**, 14521–14526 (2011).
- J. T. Kerr *et al.*, CLIMATE CHANGE. Climate change impacts on bumblebees converge across continents. *Science* **349**, 177–180 (2015).
- H. Tian *et al.*, Scale-dependent climatic drivers of human epidemics in ancient China. *Proc. Natl. Acad. Sci. U.S.A.* **114**, 12970–12975 (2017).

17. N. Mieszzkowska, H. Sugden, L. B. Firth, S. J. Hawkins, The role of sustained observations in tracking impacts of environmental change on marine biodiversity and ecosystems. *Philos Trans A Math Phys Eng Sci* **372**, 20130339 (2014).
18. J. B. Jackson *et al.*, Historical overfishing and the recent collapse of coastal ecosystems. *Science* **293**, 629–637 (2001).
19. M. W. Tingley, M. S. Koo, C. Moritz, A. C. Rush, S. R. Beissinger, The push and pull of climate change causes heterogeneous shifts in avian elevational ranges. *Glob. Change Biol.* **18**, 3279–3290 (2012).
20. B. T. Bestelmeyer *et al.*, Analysis of abrupt transitions in ecological systems. *Ecosphere* **2**, 1–26 (2011).
21. T. W. Swetnam, C. D. Allen, J. L. Betancourt, Applied historical ecology: Using the past to manage for the future. *Ecol. Appl.* **9**, 1189–1206 (1999).
22. A. Angerbjörn, M. Tannerfeldt, H. Lundberg, Geographical and temporal patterns of lemming population dynamics in Fennoscandia. *Ecography* **24**, 298–308 (2001).
23. L. McClenachan, A. B. Cooper, M. G. McKenzie, J. A. Drew, The importance of surprising results and best practices in historical ecology. *Bioscience* **65**, 932–939 (2015).
24. D. Munro, A. Fowler, Testing the credibility of historical newspaper reporting of extreme climate and weather events. *N. Z. Geog.* **70**, 153–164 (2014).
25. D. Lazer, R. Kennedy, G. King, A. Vespignani, Big data. The parable of Google Flu: Traps in big data analysis. *Science* **343**, 1203–1205 (2014).
26. L. McClenachan, Historical declines of goliath grouper populations in South Florida, USA. *Endanger. Species Res.* **7**, 175–181 (2009).
27. C. W. Lackey, J. P. Beckmann, J. Sedinger, Bear historical ranges revisited: Documenting the increase of a once-extirpated population in Nevada. *J. Wildl. Manage.* **77**, 812–820 (2013).
28. G. H. Endfield, Historical narratives of weather extremes in the UK. *Geography* **101**, 93–99 (2016).
29. M. del R Prieto, R. Herrera, P. Dussel, Historical evidences of streamflow fluctuations in the Mendoza River, Argentina, and their relationship with ENSO. *Holocene* **9**, 473–481 (1999).
30. E. Liang *et al.*, The 1920s drought recorded by tree rings and historical documents in the semi-arid and arid areas of northern China. *Clim. Change* **79**, 403–432 (2006).
31. Ó. A. Do, M. J. Roxo, Drought events in Southern Portugal from the 12th to the 19th centuries: Integrated research from descriptive sources. *Nat. Hazards* **47**, 55–63 (2008).
32. G. McKeon, W. Hall, B. Henry, G. Stone, I. Watson, *Pasture Degradation and Recovery in Australia's Rangelands: Learning from History* (Queensland Department of Natural Resources, Mines and Energy, 2014), 256 pp.
33. N. C. W. Beadle, *The Vegetation and Pastures of Western New South Wales with Special Reference to Soil Erosion* (Department of Conservation of New South Wales, Sydney, 1948), 281 pp.
34. S. R. Cattle, The case for a southeastern Australian Dust Bowl, 1895–1945. *Aeolian Res.* **21**, 1–20 (2016).
35. B. Semple, M. Rankin, T. Koen, G. Geeves, A note on tree deaths during the current (2001–?) drought in South-eastern Australia. *Aust. Geogr.* **41**, 391–401 (2010).
36. D. C. Verdon-Kidd, A. S. Kiem, Nature and causes of protracted droughts in southeast Australia: Comparison between the Federation, WWII, and Big Dry droughts. *Geophys. Res. Lett.* **36**, L22707 (2009).
37. G. Matusick, K. X. Ruthrof, N. C. Brouwers, B. Dell, G. S. J. Hardy, Sudden forest canopy collapse corresponding with extreme drought and heat in a mediterranean-type eucalypt forest in southwestern Australia. *Eur. J. For. Res.* **132**, 497–510 (2013).
38. B. Godfree *et al.*, Historical reconstruction unveils the risk of mass mortality and ecosystem collapse during pancontinental megadrought. CSIRO. <https://data.csiro.au/collections/#collection/Clsiro:40458v1/Dltrue>. Deposited 1 July 2019.
39. S. J. Jeffrey, J. O. Carter, K. B. Moodie, A. R. Beswick, Using spatial interpolation to construct a comprehensive archive of Australian climate data. *Environ. Model. Softw.* **16**, 309–330 (2001).
40. M. Freund, B. J. Henley, D. J. Karoly, K. J. Allen, P. J. Baker, Multi-century cool- and warm-season rainfall reconstructions for Australia's major climatic regions. *Clim. Past* **13**, 1751–1770 (2017).
41. E. Van Gorsel *et al.*, Carbon uptake and water use in woodlands and forests in southern Australia during an extreme heat wave event in the “Angry Summer” of 2012/2013. *Biogeosciences* **13**, 5947–5964 (2016).
42. C. C. Ummenhofer *et al.*, What causes southeast Australia's worst droughts? *Geophys. Res. Lett.* **36**, L04706 (2009).
43. P. P. Hesse, R. L. Simpson, Variable vegetation cover and episodic sand movement on longitudinal desert sand dunes. *Geomorphology* **81**, 276–291 (2006).
44. A. Dai *et al.*, The recent Sahel drought is real. *Int. J. Climatol.* **24**, 1323–1331 (2004).
45. D. M. Olson *et al.*, Terrestrial ecoregions of the world: A new map of life on Earth. *Bioscience* **51**, 933–938 (2001).
46. R. Thackway, I. D. Cresswell, *An Interim Biogeographic Regionalisation for Australia: A Framework for Setting Priorities in the National Reserves System Cooperative Program* (Australian Nature Conservancy Agency, Canberra, ACT, 1995).
47. R. Guimera, L. A. Nunes Amaral, Functional cartography of complex metabolic networks. *Nature* **433**, 895–900 (2005).
48. N. J. Bloomfield, N. Knerr, F. Encinas-Viso, A comparison of network and clustering methods to detect biogeographical regions. *Ecography* **41**, 1–10 (2018).
49. C. E. González-Orozco *et al.*, Phylogenetic approaches reveal biodiversity threats under climate change. *Nat. Clim. Chang.* **12**, 1110–1114 (2016).
50. B. D. Mishler *et al.*, Phylogenetic measures of biodiversity and neo- and paleo-endemism in Australian *Acacia*. *Nat. Commun.* **5**, 4473 (2014).
51. G. Dolman, L. Joseph, Evolutionary history of birds across southern Australia: Structure, history and taxonomic implications of mitochondrial DNA diversity in an ecologically diverse suite of species. *Emu* **115**, 35–48 (2015).
52. K. H. Wyrwoll, B. Dong, P. Valdes, On the position of southern hemisphere westerlies at the Last Glacial Maximum: An outline of AGCM simulation results and evaluation of their implications. *Quat. Sci. Rev.* **19**, 881–898 (2000).
53. M. Byrne, Evidence for multiple refugia at different time scales during Pleistocene climatic oscillations in southern Australia inferred from phylogeography. *Quat. Sci. Rev.* **27**, 2576–2585 (2008).
54. A. Toon, P. B. Mather, A. M. Baker, K. L. Durrant, J. M. Hughes, Pleistocene refugia in an arid landscape: Analysis of a widely distributed Australian passerine. *Mol. Ecol.* **16**, 2525–2541 (2007).
55. R. Godfree *et al.*, Multiscale topoeconomic heterogeneity increases resilience and resistance of a dominant grassland species to extreme drought and climate change. *Glob. Change Biol.* **17**, 943–958 (2011).
56. E. Stodart, I. Parer, *Colonisation of Australia by the Rabbit *Oryctolagus cuniculus* (L.)* (Commonwealth Scientific and Industrial Research Organisation, Canberra, 1988).
57. G. K. Himes Boor, C. B. Schultz, E. E. Crone, W. F. Morris, Mechanism matters: The cause of fluctuations in boom-bust populations governs optimal habitat restoration strategy. *Ecol. Appl.* **28**, 356–372 (2018).
58. J. Terborgh *et al.*, Ecological meltdown in predator-free forest fragments. *Science* **294**, 1923–1926 (2001).
59. A. Glen, J. Short, The control of dingoes in New South Wales in the period 1883–1930 and its likely impact on their distribution and abundance. *Aust. Zool.* **31**, 432–442 (2000).
60. C. Barnard, Bird life as affected by drought. *Emu* **16**, 234–236 (1916).
61. L. Zwarts, R. G. Bijlsma, J. van der Kamp, Large decline of birds in Sahelian rangelands due to loss of woody cover and soil seed bank. *J. Arid Environ.* **155**, 1–15 (2018).
62. A. A. Burbidge, N. L. McKenzie, Patterns in the modern decline of Western Australia's vertebrate fauna: Causes and conservation implications. *Biol. Conserv.* **50**, 143–198 (1989).
63. J. D. Koehn “The loss of valuable Murray cod in fish kills: A science and management perspective” in *Management of Murray Cod in the Murray-Darling Basin: Statement, Recommendations and Supporting Papers*, M. Lintermans, B. Phillips, Eds. (Murray-Darling Basin Commission, Canberra City, Australia, 2004), pp. 3–4.
64. D. Lindenmayer, C. Messier, C. Sato, Avoiding ecosystem collapse in managed forest ecosystems. *Front. Ecol. Environ.* **14**, 561–568 (2016).
65. A. S. MacDougall, K. S. McCann, G. Gellner, R. Turkington, Diversity loss with persistent human disturbance increases vulnerability to ecosystem collapse. *Nature* **494**, 86–89 (2013).
66. J. A. Rowland *et al.*, Selecting and applying indicators of ecosystem collapse for risk assessments. *Conserv. Biol.* **32**, 1233–1245 (2018).
67. New South Wales, “Report of the Royal Commission to inquire into the conditions of the Crown tenants, Western Division of New South Wales” in *Votes and Proceedings* (Government Printer, Sydney, NSW, 1901), vol. 4.
68. H. G. Barnard, Effects of droughts on bird-life in central Queensland. *Emu* **27**, 35–37 (1927).
69. D. Le Souef, Queensland Notes. *Emu* **18**, 43–49 (1918).
70. B. D. Cooke, R. C. Sorriquer, Do dingoes protect Australia's small mammal fauna from introduced mesopredators? Time to consider history and recent events. *Food Webs* **12**, 95–106 (2017).
71. M. D. McCue, Starvation physiology: Reviewing the different strategies animals use to survive a common challenge. *Comp. Biochem. Physiol. A Mol. Integr. Physiol.* **156**, 1–18 (2010).
72. K. A. Nagy, I. A. Girard, T. K. Brown, Energetics of free-ranging mammals, reptiles, and birds. *Annu. Rev. Nutr.* **19**, 247–277 (1999).
73. N. R. Bond, P. S. Lake, A. H. Arthington, The impacts of drought on freshwater ecosystems: An Australian perspective. *Hydrobiologia* **600**, 3–16 (2008).
74. S. C. Cunningham *et al.*, A robust technique for mapping vegetation condition across a major river system. *Ecosystems* **12**, 207–219 (2009).
75. R. T. Kingsford, Ecological impacts of dams, water diversions and river management on floodplain wetlands in Australia. *Austral Ecol.* **25**, 109–127 (2000).
76. M. Byrne *et al.*, Decline of a biome: Evolution, contraction, fragmentation, extinction and invasion of the Australian mesic zone biota. *J. Biogeogr.* **38**, 1635–1656 (2011).
77. D. Chu, R. Strand, R. Fjelland, Theories of complexity. *Complexity* **8**, 19–30 (2003).
78. J. A. Estes *et al.*, Trophic downgrading of planet Earth. *Science* **333**, 301–306 (2011).
79. J. Tibby, J. J. Tyler, C. Barr, Post little ice age drying of eastern Australia conflates understanding of early settlement impacts. *Quat. Sci. Rev.* **202**, 45–52 (2018).
80. Z. Hochman, D. L. Gobbett, H. Horan, Climate trends account for stalled wheat yields in Australia since 1990. *Glob. Change Biol.* **23**, 2071–2081 (2017).
81. M. Saft, A. W. Western, L. Zhang, M. C. Peel, N. J. Potter, The influence of multiyear drought on the annual rainfall-runoff relationship: An Australian perspective. *Water Resour. Res.* **51**, 2444–2463 (2015).
82. D. G. Kirono, K. J. Hennessy, M. R. Grose, Increasing risk of months with low rainfall and high temperature in southeast Australia for the past 150 years. *Clim. Risk Manage.* **16**, 10–21 (2017).
83. R. S. Bivand, E. Pebesma, V. Gómez-Rubio, *Applied Spatial Data Analysis with R* (Springer, New York, NY, 2013), 405 pp.
84. C. Brundston, L. Comber, *An Introduction to R for Spatial Analysis and Mapping* (Sage Publications Ltd., London, 2015), 343 pp.